Geodesic Acoustic Mode with the Existence of a Poloidal Shock Structure

Naohiro KASUYA and Kimitaka ITOH

National Institute for Fusion Science, 322-6 Oroshi-cho, Toki 509-5292, Japan

In H-mode plasmas, two-dimensionally steep structures of the potential and density are formed, when a large poloidal flow exists, and its formation mechanism has been studied for quantitative understanding of the particle transport in the H-mode transport barriers. Extension of the previous two-dimensional model is carried out to investigate parallel flow dynamics, when potential and density distributions do not satisfy the Boltzmann relation. The extended model includes the generation mechanism of a poloidal shock structure and a geodesic acoustic mode, and their competitive formation can be studied.

Keywords: poloidal shock structure, geodesic acoustic mode, H mode, poloidal asymmetry, structural formation

1. Introduction

A variety of structures are formed in the toroidal plasmas, and their formation mechanism is one of the keys to understand the transport phenomena. The typical example appears in the high-confinement mode (H mode) [1]. The steep radial electric field plays an important role for turbulent suppression in H-mode transport barriers [2]. In addition, a poloidally steep structure can be formed, associated with a large poloidal flow. Theories have predicted that the poloidal shock can appear in H-mode plasmas [3,4]. The poloidal shock structure is a steady density or potential jump in the poloidal direction, resulting from the plasma compressibility and the inhomogeneity of the magnetic field by the toroidicity, and is important, because it induces radial particle fluxes to accelerate the density pedestal formation on the L/H transition [5]. Some experiments have indicated the existence of poloidal asymmetry [6,7]. Therefore, it is important to understand the formation mechanism of H-modes by analyzing the two-dimensional (2-D) electric field structure.

We have extended the one-dimensional (1-D) model in tokamak H modes to give 2-D structures, taking into consideration of coupling between different magnetic surfaces by shear viscosity, and obtained 2-D potential and density structures in edge transport barriers [5]. Our evaluation clarifies the non-negligibility of the particle transport arising from poloidal asymmetry, and the self-consistent mechanism of the density pedestal formation on the L/H transition [8].

In this paper, extensions of the previous 2-D model are carried out to investigate two effects on the structural formation, i.e., the deviation from the Boltzmann relation and the parallel flow dynamics. The distribution of the potential and density different from the Boltzmann relation contributes to induce a particle pinch [8], and the parallel flow dynamics is important to obtain the flow pattern, which contributes to the structural formation [2]. These extensions enable to analyze the geodesic acoustic mode (GAM) [9], which is the oscillatory zonal flow, caused by compressibility of the E × B flow in the presence of the geodesic magnetic curvature [10]. The zonal flow nonlinearly interacts with turbulence and determines the transport level. Therefore, many experimental observations have been made to clarify the role of the zonal flow in plasma confinements [11]. Both the poloidal shock and the geodesic acoustic mode induce density asymmetry in the magnetic flux surface, so their competition must be examined to deepen our understanding of the transport barrier physics.

The paper is organized as follows. The derivation of the model equations is described in Sec. 2. In Sec. 3, the extreme cases with a large and small poloidal flow are shown to deduce the formation mechanism of the poloidal shock and the GAM. The summary is presented in Sec. 4.

2. Set of Model Equations

For analyzing the potential, the density and the flow velocity, a set of fluid equations consists of the momentum conservation equation, the continuity equation of the density, the charge conservation equation, and the Ohm's law:

$$m_i n \frac{d}{dt}\vec{V}_i = \vec{J}\times\vec{B} - \vec{\nabla}(p_i + p_e) - \vec{\nabla}\cdot\vec{\pi}_i , \quad (1)$$

$$\frac{\partial n}{\partial t} + \vec{\nabla}\cdot\left(n\vec{V}_i\right) = 0 , \quad (2)$$

$$\vec{\nabla}\cdot\vec{J} = 0 , \quad (3)$$

$$\vec{E} + \vec{V}\times\vec{B} = 0 , \quad (4)$$

where m_i is the ion mass, $\vec{V}$ is the flow velocity, $\vec{J}$ is the current, p is the pressure, $\vec{\pi}$ is the viscosity. We assume density $n = n_i = n_e$ for simplicity, where n_i and n_e are the ion and electron density, respectively. We consider a large aspect ratio tokamak with a circular cross-section and the coordinates (r, θ, ϕ) are used (r: radius, θ: poloidal angle, ϕ:

author's e-mail: kasuya@nifs.ac.jp

toroidal angle). The magnetic field is taken to be

$$\vec{B} = \frac{1}{1+\varepsilon\cos\theta}\begin{pmatrix} 0 \\ B_{\mathrm{p}0}(r) \\ B_{\phi 0} \end{pmatrix}, \tag{5}$$

where ε is the inverse aspect ration. Using Eq. (4), the flow velocity can be written to be

$$\vec{V} = \vec{V}_{//} + \frac{\vec{E}\times\vec{B}}{B^2} = \begin{pmatrix} -\frac{1}{rB}\frac{\partial\Phi}{\partial\theta} \\ \frac{KB_{\mathrm{p}}}{n} \\ \frac{KB_{\phi}}{n} - \frac{1}{B_{\mathrm{p}}}\frac{\partial\Phi}{\partial r} \end{pmatrix}, \tag{6}$$

where

$$K \equiv nV_{\mathrm{p}}/B_{\mathrm{p}}, \tag{7}$$

and Φ is the potential. Using Eq. (6), Eq. (2), the poloidal and parallel component of Eq. (1) are given to be

$$\frac{\partial n}{\partial t} - \frac{\partial}{\partial r}\left(\frac{n}{rB}\frac{\partial\Phi}{\partial\theta}\right) + \frac{1}{r}\frac{\partial}{\partial\theta}\left(KB_{\mathrm{p}}\right) = 0, \tag{8}$$

$$\begin{aligned} &{B_{\mathrm{p}}}^2\frac{\partial}{\partial t}\left(\frac{K}{n}\right) - \frac{n}{KrB}\frac{\partial\Phi}{\partial\theta}\frac{\partial}{\partial r}\left[\frac{1}{2}\left(\frac{KB_{\mathrm{p}}}{n}\right)^2\right] + \frac{B_{\mathrm{p}}}{r}\frac{\partial}{\partial\theta}\left[\frac{1}{2}\left(\frac{KB_{\mathrm{p}}}{n}\right)^2\right] \\ &= \frac{1}{m_{\mathrm{i}}}\frac{JB_{\mathrm{p}}B_{\phi}}{n} - \frac{1}{m_i}\frac{B_{\mathrm{p}}}{r}\frac{\partial}{\partial\theta}\left(\frac{\bar{p}_e}{\bar{n}}\ln n + \frac{5\bar{p}_i}{2\bar{n}^{5/3}}n^{2/3}\right) \\ &\quad - \frac{1}{m_{\mathrm{i}}}\left(\frac{\vec{B}_{\mathrm{p}}\cdot\vec{\nabla}\cdot\vec{\pi}_{\mathrm{i}}}{n}\right)_{\mathrm{bulk}} - \frac{1}{m_{\mathrm{i}}}\left(\frac{\vec{B}_{\mathrm{p}}\cdot\vec{\nabla}\cdot\vec{\pi}_{\mathrm{i}}}{n}\right)_{\mathrm{shear}}, \end{aligned} \tag{9}$$

$$\begin{aligned} &B^2\frac{\partial}{\partial t}\left(\frac{K}{n}\right) - \frac{B_{\phi}}{B_{\mathrm{p}}}\frac{\partial}{\partial t}\frac{\partial\Phi}{\partial r} - \frac{n}{KrB}\frac{\partial\Phi}{\partial\theta}\frac{\partial}{\partial r}\left[\frac{1}{2}\left(\frac{KB}{n}\right)^2\right] \\ &+ \frac{B_{\mathrm{p}}}{r}\frac{\partial}{\partial\theta}\left[\frac{1}{2}\left(\frac{KB}{n}\right)^2\right] + \frac{B_{\phi}}{rB}\frac{\partial\Phi}{\partial\theta}\frac{\partial}{\partial r}\left[\frac{B}{B_{\mathrm{p}}B_{\phi}}\frac{\partial\Phi}{\partial r}\right] \\ &- \frac{KB_{\mathrm{p}}B_{\phi}}{nr}\frac{\partial}{\partial\theta}\left[\frac{B}{B_{\mathrm{p}}B_{\phi}}\frac{\partial\Phi}{\partial r}\right] \\ &= -\frac{B_{\mathrm{p}}}{m_{\mathrm{i}}r}\frac{\partial}{\partial\theta}\left(\frac{\bar{p}_e}{\bar{n}}\ln n + \frac{5}{2}\frac{\bar{p}_i}{\bar{n}^{5/3}}n^{2/3}\right) \\ &\quad - \frac{1}{m_{\mathrm{i}}n}\left(\vec{B}\cdot\vec{\nabla}\cdot\vec{\pi}_{\mathrm{i}}\right)_{\mathrm{bulk}} - \frac{1}{m_{\mathrm{i}}n}\left(\vec{B}\cdot\vec{\nabla}\cdot\vec{\pi}_{\mathrm{i}}\right)_{\mathrm{shear}}, \end{aligned} \tag{10}$$

respectively. Isothermal electrons and adiabatic ions are assumed. The viscosity of ions $\vec{\pi}_{\mathrm{i}}$ is divided into two terms: the bulk viscosity given by a neoclassical process [12], and shear viscosity given by an anomalous process [2]. The forms of viscosity terms are represented in Ref. [13].

The 2-D structures of the potential, the density and the flow velocity are obtained. These variables are divided into the average part and the perturbation part: $f = f_0(r) + f_1(r, \theta)$, where f represents each quantity. The variable K is replaced by M_{p}, which corresponds to the poloidal Mach number and defined as

$$M_{\mathrm{p}} \equiv \frac{KB_0}{\bar{n}\mathrm{v}_{\mathrm{ti}}C_{\mathrm{r}}}. \tag{11}$$

where $\mathrm{v}_{\mathrm{ti}} = \sqrt{2T_{\mathrm{i}}/m_{\mathrm{i}}}$, ${C_{\mathrm{r}}}^2 = 5/6 + T_{\mathrm{e}}/(2T_{\mathrm{i}})$, T_{i} and T_{e} is the ion and electron temperature, respectively. Here, the shock ordering, which is the perturbations to be $O(\varepsilon^{1/2})$, is adopted. In the case in which $M_{\mathrm{p}} \sim 1$, the steep structure in the poloidal direction is formed, and the perturbations become larger than $O(\varepsilon)$. The set of equations for obtaining $M_{\mathrm{p}0}$, $M_{\mathrm{p}1}$, Φ_1, n_1 is derived from Eqs. (8-10), assuming V_{r} / V_{p} << 1, which is satisfied, even if a strong poloidal shock exists:

$$\frac{\partial\chi}{\partial\tau} = M_{\mathrm{p}0}\varepsilon\sin\theta - \frac{\partial M_{\mathrm{p}1}}{\partial\theta}, \tag{12}$$

$$\frac{{B_{\mathrm{p}0}}^3{\mathrm{v}_{\mathrm{ti}}}^2{C_r}^2}{{B_0}^2 r}\frac{\partial M_{\mathrm{p}0}}{\partial\tau} = \frac{1}{m_{\mathrm{i}}}\left\langle\frac{JB_{\mathrm{p}}B_{\phi}}{n}\right\rangle - \frac{1}{m_{\mathrm{i}}}\left\langle\frac{\vec{B}_{\mathrm{p}}\cdot\vec{\nabla}\cdot\vec{\pi}_{\mathrm{i}}}{n}\right\rangle_{\mathrm{bulk}} - \frac{1}{m_{\mathrm{i}}}\left\langle\frac{\vec{B}_{\mathrm{p}}\cdot\vec{\nabla}\cdot\vec{\pi}_{\mathrm{i}}}{n}\right\rangle_{\mathrm{shear}}, \tag{13}$$

$$\begin{aligned} \frac{\partial E_1}{\partial\tau} &= -\hat{\mu}r^2\frac{B_0}{B_{\mathrm{p}0}}\frac{\partial^2}{\partial r^2}\left\{M_{\mathrm{p}0}\left[\exp(-\chi)-1\right]\right\} \\ &+ \frac{2}{3}D\exp(-\chi)\frac{\partial^2\chi}{\partial\theta^2} \\ &+ \left(1-{M_{\mathrm{p}0}}^2\right)\frac{\partial\chi}{\partial\theta} + 2A\frac{\partial\chi^2}{\partial\theta} \\ &- \varepsilon\left\{D - \hat{\mu}\frac{B_0}{B_{\mathrm{p}0}}\left[2r^2\frac{\partial^2 M_{\mathrm{p}0}}{\partial r^2} + 4r\frac{\partial M_{\mathrm{p}0}}{\partial r} - 2M_{\mathrm{p}0}\right]\right\} \\ &\times\cos\theta + 2\varepsilon{M_{\mathrm{p}0}}^2\sin\theta \\ &- \left(\chi - \frac{\chi^2}{2} + 2\varepsilon\cos\theta\right)\frac{\partial M_{\mathrm{p}0}}{\partial\tau} \\ &+ \frac{\partial M_{\mathrm{p}1}}{\partial\tau} - M_{\mathrm{p}0}\exp(-\chi)\frac{\partial\chi}{\partial\tau}, \end{aligned} \tag{14}$$

$$\begin{aligned} \frac{\partial M_{\mathrm{p}1}}{\partial\tau} &= M_{\mathrm{p}0}\frac{\partial\chi}{\partial\tau} + \chi\frac{\partial M_{\mathrm{p}0}}{\partial\tau} \\ &- \frac{B_0}{B_{\mathrm{p}0}}\frac{1}{\mathrm{v}_{\mathrm{ti}}C_{\mathrm{r}}}\frac{\partial}{\partial\theta}\left(M_{\mathrm{p}1} - M_{\mathrm{p}0}\varepsilon\cos\theta - \chi M_{\mathrm{p}0} - \chi M_{\mathrm{p}1} + \frac{\chi^2}{2}M_{\mathrm{p}0}\right) \\ &- \frac{B_0}{B_{\mathrm{p}0}}\frac{1}{\mathrm{v}_{\mathrm{ti}}C_{\mathrm{r}}}\varepsilon\cos\theta\frac{\partial}{\partial\theta}\left(M_{\mathrm{p}1} - M_{\mathrm{p}0}\varepsilon\cos\theta - \chi M_{\mathrm{p}0}\right) \\ &- \frac{{B_0}^2}{{B_{\mathrm{p}0}}^2}\left[\frac{\partial}{\partial\theta}\left(\chi + \frac{5}{18}\frac{1}{{C_r}^2}\chi^2\right) + \varepsilon\cos\theta\frac{\partial\chi}{\partial\theta}\right] \\ &+ \frac{{B_0}^2 r}{{B_{\mathrm{p}0}}^3{\mathrm{v}_{\mathrm{ti}}}^2{C_{\mathrm{r}}}^2}\frac{1}{m_{\mathrm{i}}} \\ &\times\left[\frac{JB_{\mathrm{p}}B_{\phi}}{n} - \left(\frac{\vec{B}_{\mathrm{p}}\cdot\vec{\nabla}\cdot\vec{\pi}_{\mathrm{i}}}{n}\right)_{\mathrm{bulk}} - \left(\frac{\vec{B}_{\mathrm{p}}\cdot\vec{\nabla}\cdot\vec{\pi}_{\mathrm{i}}}{n}\right)_{\mathrm{shear}}\right], \end{aligned} \tag{15}$$

where

$$\chi = \ln(n/\bar{n}), \tag{16}$$

$$E_1 = \frac{1}{B_{\mathrm{p}0}\mathrm{v}_{\mathrm{ti}}C_{\mathrm{r}}}\frac{\partial\Phi_1}{\partial r}, \tag{17}$$

$$D = \frac{4\sqrt{\pi}}{3}\frac{I_{\mathrm{ps}}K_0B_0}{\bar{n}\mathrm{v}_{\mathrm{ti}}{C_{\mathrm{r}}}^2}, \tag{18}$$

$$A = \frac{{M_{\mathrm{p0}}}^2}{2} + \frac{5}{36}\frac{1}{{C_{\mathrm{r}}}^2}, \tag{19}$$

$\hat{\mu}$ is the shear viscosity coefficient, and the form of I_{ps} is represented in Eq. (10) of Ref. [4], and depends on M_{p} and the collision frequency [14]. The variables n_1 and Φ_1 are replaced by χ and E_1 in this set, respectively. Time t is normalized as $\tau = t/t_{\mathrm{p}}$, where

$$t_{\mathrm{p}} = \frac{B_0 r}{B_{\mathrm{p0}} \mathrm{v}_{\mathrm{ti}} C_{\mathrm{r}}}. \tag{20}$$

Eqs. (13) and (14) are the flux surface average and the 2nd order of Eq. (9), respectively. Current J is obtained from Eq. (3), which includes polarization current $\varepsilon_0 \varepsilon_\perp \partial E_{\mathrm{r}}/\partial t$, and external components as driven by an electrode, orbit losses, etc. [15], where ε_0 is the vacuum susceptibility, and $\varepsilon_\perp$ is the perpendicular dielectric constant of a toroidal plasma, which depends on the flow pattern and is of the order of $c^2 / \mathrm{v_A}^2$, where $\mathrm{v_A}$ is the Alfvén velocity [2].

3. Formation Mechanisms of Poloidal Asymmetry

A set of model equations consists of Eqs. (12-15). This extended model includes the generation mechanism of the poloidal shock structure and the GAM. Some simplified cases are described to depict the fundamental mechanisms in this section.

3.1. Poloidal Shock Structure

The key mechanism for poloidal shock formation is in the momentum conservation Eq. (1). With the existence of the large poloidal flow, nonlinear effects in the convective derivative and the density gradient generate the poloidal shock structure by coupling with toroidicity. Assumption of Boltzmann relation

$$n = \bar{n} \exp \frac{e\Phi_1}{T_{\mathrm{i}}} \tag{21}$$

and strong toroidal flow damping

$$V_\phi = 0, \tag{22}$$

which makes M_{p} to be proportional to the radial electric field, give a simplified set of equations. Equation (14) is given to be

$$\begin{aligned} M_{\mathrm{p0}} \exp(-\chi)\frac{\partial \chi}{\partial \tau} &= -\hat{\mu} r^2 \frac{B_0}{B_{\mathrm{p0}}} \frac{\partial^2}{\partial r^2} \left\{ M_{\mathrm{p0}} [\exp(-\chi) - 1] \right\} \\ &+ \frac{2}{3} D \exp(-\chi) \frac{\partial^2 \chi}{\partial \theta^2} + \left(1 - {M_{\mathrm{p0}}}^2\right) \frac{\partial \chi}{\partial \theta} + 2A \frac{\partial \chi^2}{\partial \theta} \\ &- \left(\chi - \frac{\chi^2}{2} + 2\varepsilon \cos\theta \right) \frac{\partial M_{p0}}{\partial \tau} \\ &- \varepsilon \left\{ D - \hat{\mu} \frac{B_0}{B_{\mathrm{p0}}} \left[2r^2 \frac{\partial^2 M_{\mathrm{p0}}}{\partial r^2} + 4r \frac{\partial M_{\mathrm{p0}}}{\partial r} - 2M_{\mathrm{p0}} \right] \right\} \cos\theta \\ &+ 2\varepsilon {M_{\mathrm{p0}}}^2 \sin\theta \end{aligned} \tag{23}$$

In this case, an iterative process can be taken to obtain the solution, i.e., time evolution of the 2-D structure is calculated from Eq. (23) by substituting M_{p0} obtained by Eq. (13). Then, using Boltzmann relation (21), the potential profile is obtained.

Figure 1 shows the example of the 2-D structure (the detail of the simulation parameters is presented in Ref. [8]). With a prescribed inhomogeneous density profile as shown in Fig. 1 (a), normal and enhanced radial electric field branches are taken in the small and large gradient regions (near the boundary r - a = -5, 0 [cm], where $r = a$ is the position of the

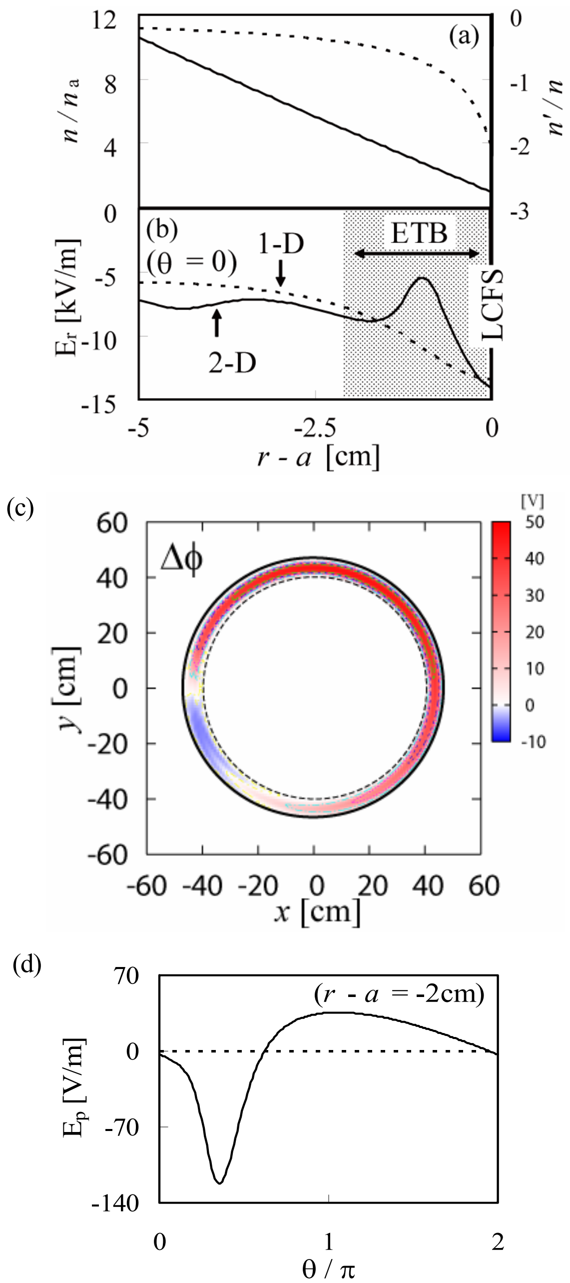

Fig.1 (a) Radial profiles of the density (n) normalized by the density at the edge $r = a$ (n_{a}) (solid line), and the reciprocal of the density scale length (dashed line). (b) Radial profiles of the radial electric field at $\theta = 0$ (Solutions of the 1-D and 2-D model), and (c) 2-D structure of the potential perturbation. (d) Poloidal profile of the poloidal electric field at r - a = -2 [cm] in spontaneous H mode.

last closed flux surface), respectively, and a critical layer is formed between these regions (at r - a ~ -1 [cm]). The steep gradient of the radial electric field is formed in this layer. The radial electric field profiles in the radial direction are shown in Fig. 1 (b) by solving the 1-D and 2-D model. The 2-D structure of the potential perturbation is shown in Fig. 1 (c). There exists a poloidal structure, and Fig. 1 (d) shows the poloidal electric field profile. The poloidal shock structure exists at $\theta \sim 0.2\pi - 0.5\pi$ in this case.

3.2. Geodesic Acoustic Mode

The GAM exists in the toroidal plasmas by coupling between the (m, n) = (0, 0) electrostatic potential and (1, 0) sideband density perturbation, where m and n are the poloidal and toroidal mode number, respectively [10]. Taking the ordering that perturbations have $O(\varepsilon)$ with a small poloidal flow, Eq. (12), flux surface average of Eqs. (13) + (14) and Eq. (15) with $\hat{\mu} = 0$ are give to be

$$\frac{\partial \chi}{\partial \tau} = M_{\mathrm{p0}} \varepsilon \sin\theta - \frac{\partial M_{\mathrm{p1}}}{\partial \theta}, \tag{24}$$

$$\frac{\partial M_{\mathrm{p0}}}{\partial \tau} = -\frac{B_0^{\,2}}{B_{\mathrm{p0}}^{\,2}} \left\langle \varepsilon \cos\theta \frac{\partial \chi}{\partial \theta} \right\rangle, \tag{25}$$

$$\frac{\partial M_{\mathrm{p1}}}{\partial \tau} = -\frac{\partial \chi}{\partial \theta}, \tag{26}$$

respectively. This set of equations describes the GAM oscillation. If the density perturbation has a $\sin\theta$ dependency

$$\chi = \chi_{\mathrm{r}}(r,t)\sin\theta, \tag{27}$$

Eqs. (24-26) gives the dispersion relation

$$\Omega^2 - \frac{\varepsilon^2}{2} \frac{B_0^{\,2}}{B_{\mathrm{p0}}^{\,2}} - k_\theta^{\,2} = 0, \tag{28}$$

where Ω is the oscillation frequency and k_θ is the wave number in the poloidal direction. The time is normalized by t_{p} shown in Eq (20), and the frequency in real unit is given to be

$$\omega = \frac{C_{\mathrm{r}}}{\sqrt{2}} \frac{\mathrm{v}_{\mathrm{ti}}}{R} \left(1 + \frac{2k_\theta^{\,2}}{q^2} \right), \tag{29}$$

where q is the safety factor.

4. Summary

The extended set of fluid equations, which consists of the momentum conservation equation, the continuity equation of the density, the charge conservation equation, and the Ohm's law, is derived to obtain 2-D structures of the potential, the density and the flow velocity in H-mode transport barriers. This model includes the generation mechanism of the poloidal shock structure and the GAM, and their competitive formation can be studied. The derivation is the first step to analyze the multi-dimensionality of transport in the toroidal plasmas, which gives quantitative understandings of the transport barrier physics.

Acknowledgement

Authors acknowledge discussions with Prof. S.-I. Itoh, Prof. M. Yagi, Prof. A. Fukuyama and Prof. Y. Takase. This work is partly supported by the Grant-in-Aid for Specially-Promoted Research (16002005) and for Scientific Research (19360418) of MEXT, by Research Fellowships of the Japan Society for the Promotion of Science for Young Scientists, and by the collaboration programs of NIFS (NIFS06KDAD005, NIFS07KOAP017) and of RIAM of Kyushu University.

References

[1] F. Wagner *et al.*, Phys. Rev. Lett. **49**, 1408 (1982).
[2] K. Itoh, S.-I. Itoh and A. Fukuyama, *Transport and Structural Formation in Plasmas* (IOPP, Bristol, 1999).
[3] T. Taniuti, H. Moriguchi, Y. Ishii, K. Watanabe and M. Wakatani, J. Phys. Soc. Jpn. **61**, 568 (1992).
[4] K. C. Shaing, R. D. Hazeltine and H. Sanuki, Phys. Fluids B **4**, 404 (1992).
[5] N. Kasuya and K. Itoh, Phys. Rev. Lett. **94**, 195002 (2005).
[6] A. Mohri and M. Fujiwara, Nucl. Fusion **14**, 67 (1974).
[7] R. J. Taylor, P. Pribyl, G. R. Tynan and B. C. Wells, in *Proc. of 15th International Conference on Plasma Physics and Controlled Nuclear Fusion Research, Seville, 1994* (IAEA, Vienna, 1995) Vol. 2, p. 127.
[8] N. Kasuya and K. Itoh, submitted to Nucl. Fusion (2006).
[9] N. Winsor, J. L. Johnson and J. M. Dawson, Phys. Fluids **11**, 2448 (1968).
[10] For a review, e.g. P. H. Diamond, S.-I. Itoh, K. Itoh and T. S. Hahm, Plasma Phys. Control. Fusion **47**, R35 (2005).
[11] For a review, e.g. A. Fujisawa et al., Nucl. Fusion **47**, S718 (2007).
[12] K. C. Shaing, E. C. Crume and W. A. Houlberg, Phys. Fluids B **2**, 1492 (1990).
[13] N. Kasuya and K. Itoh, J. Plasma Fusion Res. **81**, 553 (2005).
[14] N. Kasuya and K. Itoh, Phys. Plasmas **12**, 090905 (2005).
[15] N. Kasuya, K. Itoh and Y. Takase, Nucl. Fusion **43**, 244 (2003).